Median preoptic neurones projecting to the hypothalamic paraventricular nucleus respond to osmotic, circulating Ang II and baroreceptor input in the rat

Sean D. Stocker[1,2] and Glenn M. Toney[2]

[1]*Department of Physiology, University of Kentucky College of Medicine, Lexington, KY 40536-0298, USA*
[2]*Department of Physiology, University of Texas Health Science Center, San Antonio, TX 78229, USA*

The present study sought to determine whether individual neurones of the median preoptic nucleus (MnPO) with axonal projections to the hypothalamic paraventricular nucleus (MnPO-PVN) respond to osmotic, circulating angiotensin II (Ang II), and baroreceptor stimulation. Hypertonic NaCl (0.75 or 1.5 osmol l^{-1}) or Ang II (150 ng) was injected into the internal carotid artery (ICA). Baroreceptor stimulation was performed by I.V. injection of phenylephrine or sodium nitroprusside to increase or decrease arterial blood pressure, respectively. Of 65 MnPO neurones, 50 units were antidromically activated from the PVN with an average onset latency of 11.3 ± 0.7 ms. Only 9.5% of MnPO-PVN neurones were antidromically activated from the PVN bilaterally. Type I MnPO-PVN neurones ($n = 14$) responded to osmotic but not Ang II stimulation. In 79% (11/14) of these type I neurones, the response was an increase in cell discharge. Type II MnPO-PVN neurones ($n = 7$) displayed a significant increase in cell discharge in response to ICA injection of Ang II but not hypertonic NaCl. Type III MnPO-PVN neurones ($n = 16$) responded to both ICA injection of hypertonic NaCl and Ang II. In 88% (14/16) of type III neurones, osmotic and Ang II stimulation each increased cell discharge. Type IV MnPO-PVN neurones ($n = 13$) displayed no change in cell discharge in response to ICA injection of hypertonic NaCl or Ang II. Baroreceptor stimulation altered the discharge in subpopulations of type I, II and III MnPO-PVN neurones (43–63% depending on neuronal type). Only one MnPO-PVN neurone responded solely to baroreceptor stimulation (type IV). In addition, a subset of type I, II and III neurones displayed a significant correlation with sympathetic nerve activity and/or the cardiac cycle. These findings suggest that a significant population of MnPO-PVN neurones respond to osmotic and circulating Ang II stimulation and thereby represents a neural substrate through which neurohumoral inputs are integrated within the forebrain lamina terminalis.

The median preoptic nucleus (MnPO) or nucleus medianus plays an important role in cardiovascular regulation and body fluid homeostasis. It lies within the forebrain lamina terminalis adjacent to the anterior commissure and is densely innervated by two circumventricular organs, the subfornical organ and organum vasculosum of the lamina terminalis, that detect changes in circulating angiotensin II (Ang II) levels and plasma osmolality (or sodium), respectively (Johnson & Loewy, 1990; Johnson *et al.* 1996). Additionally, the MnPO has afferent connections with pontomedullary areas known to receive visceral input from arterial baroreceptors and/or cardiopulmonary receptors (Saper *et al.* 1983). In turn, MnPO neurones largely terminate onto both magnocellular and parvocellular neurones of the hypothalamic paraventricular nucleus (PVN) and supraoptic nucleus (Sawchenko & Swanson, 1983; Oldfield *et al.* 1991; Zardetto-Smith *et al.* 1993) to modulate neurohypophyseal secretion, autonomic outflow, and the ingestion of water and salt.

Lesions of the anteroventral region of the third cerebral ventricle which include the MnPO produce profound alterations in body fluid homeostasis and cardiovascular regulation. Most notably, these lesions attenuate experimentally induced thirst, vasopressin secretion and arterial hypertension in several experimental

S. D. Stocker and G. M. Toney

models associated with elevated sympathetic outflow (Johnson & Loewy, 1990). Similarly, more discrete lesions of the MnPO disrupt drinking behaviour stimulated by hyperosmolality, Ang II and hypovolemia (Mangiapane *et al.* 1983; Gardiner & Stricker, 1985; Cunningham *et al.* 1991; Cunningham *et al.* 1992), and attenuate neurohypophysial secretion of vasopressin stimulated by hyperosmolality and Ang II (Mangiapane *et al.* 1983; Gardiner *et al.* 1985). Moreover, lesion or inactivation of the MnPO attenuates centrally mediated pressor responses stimulated by Ang II or hyperosmolality (O'Neill & Brody, 1987; Yasuda *et al.* 2000). Taken together, these observations strongly suggest the MnPO may serve as a forebrain integration site for both humoral and visceral afferent information related to body fluid homeostasis and autonomic function.

Despite the potential integrative role of the MnPO, relatively few *in vivo* studies have investigated whether hyperosmolality, circulating Ang II and baroreceptor input alter the firing rates of MnPO neurones with axonal projections to the PVN (MnPO-PVN). This specific population of MnPO neurones probably plays a significant role in the responses to these challenges as the PVN is well-positioned to coordinate neuroendocrine, autonomic and behavioural responses to stress since it contains magnocellular and parvocellular neuro-endocrine and autonomic neurones. In this regard, the discharge of MnPO-PVN neurones has been reported to increase in response to hyperosmolality (Tanaka *et al.* 1995), whereas a separate study demonstrated that the firing rates of MnPO-PVN neurones decreased during baroreceptor activation produced by increases in arterial blood pressure (ABP) (Tanaka *et al.* 1993). However, there is surprisingly no data demonstrating that increases in circulating Ang II levels alter the discharge of MnPO-PVN neurones. More importantly, it is not known whether osmotic, circulating Ang II and baroreceptor inputs target distinct or identical populations of MnPO-PVN neurones. The present study used extracellular single-unit recordings *in vivo* to determine whether individual MnPO-PVN neurones are responsive to osmotic, circulating Ang II and/or baroreceptor inputs. Since the MnPO has been implicated in centrally mediated pressor responses and autonomic function (O'Neill & Brody, 1987; Yasuda *et al.* 2000), we also determined whether the discharge of these MnPO-PVN neurones was temporally correlated with sympathetic nerve activity (SNA) and the cardiac cycle.

Methods

Animals

Adult male Sprague-Dawley rats (Charles River Laboratories) weighing 300–375 g were housed in a temperature-controlled room (22–23°C) with a 14 : 10 h light–dark cycle (lights on at 7 AM). Tap water and laboratory chow (Harlan Teklad LM-485, 0.3% NaCl) were available *ad libitum* except where noted. A total of 40 rats were used for the electrophysiology investigation of MnPO neurones and an additional 3 rats were used for retrograde tract tracing experiments. All experimental and surgical procedures were approved by the Institutional Animal Care and Use Committee of the University of Texas Health Science Center at San Antonio and were performed in strict accordance with the National Institutes of Health Guide for the Care and Use of Laboratory Animals.

Experimental procedures

Rats were anaesthetized either with a mixture of α-chloralose (75 mg kg^{-1}) and urethane (750 mg kg^{-1}) given intraperitoneally or initially with 3% isoflurane (in 100% O_2) followed by an identical mixture of α-chloralose and urethane intravenously. After tracheal cannulation, rats were neuromuscularly blocked with a continuous infusion of gallamine triethiode dissolved in 5% dextrose (25 mg kg^{-1} h^{-1}, 80 μl h^{-1}, I.V.) through a femoral catheter and artificially ventilated with oxygen-enriched room air. End tidal P_{CO_2} was maintained between 4.5 and 5.5% by adjusting ventilation rate (70–100 breaths min^{-1}) and/or tidal volume (2–3 ml). Additional catheters were placed into the left brachial artery and right jugular vein for recording ABP and administration of drugs, respectively. Body temperature was maintained at 37 ± 1°C with a water-circulating pad. Mean ABP (MAP) was determined by adding one-third of the pulse pressure to diastolic blood pressure. Heart rate was derived from the peak of the QRS complex obtained from EKG leads placed in the forepaws. An adequate depth of anaesthesia was assessed by absence of a withdrawal reflex (before neuromuscular blockade) or a pressor response to foot pinch. Supplemental doses of anaesthetic (10% of initial dose, I.V.) were given as necessary.

Extracellular single-unit recordings

Rats were placed in a stereotaxic head frame and the skull was levelled between bregma and lambda. A craniotomy was performed to remove bone overlying the cortex to allow electrodes to be lowered into the MnPO and PVN. Extracellular recordings of MnPO neurones were made with an intracellular amplifier in bridge mode (AxoClamp 2B, Axon Instruments) and glass microelectrodes filled with 2% Chicago Sky Blue or 5% Neurobiotin (see 'Juxtacellular labelling' below) dissolved in isotonic saline and a tip resistance of 10–30 MΩ measured *in vivo*. The MnPO was probed for single-unit activity with the electrode down-angled 6–8 deg to gain access to the midline without moving the midsagital sinus.

The glass electrode was moved vertically in $2\,\mu$m steps with a piezoelectric micropositioning device while electrically stimulating the PVN (see 'Antidromic stimulation of the PVN' below) to identify both spontaneously active and quiescent units.

Antidromic stimulation of the PVN

To identify MnPO neurones with axonal projections to the PVN, antidromic stimulation was performed using a concentric bipolar stimulating electrode (outer tip diameter, $250\,\mu$m; Frederick Haer & Co, Bowdoinham, ME, USA) placed into the ipsilateral PVN (1.7–2.0 mm caudal to bregma, 0.5–0.7 mm lateral to midline, 7.6–7.8 mm ventral to brain surface). In some experiments, bipolar stimulating electrodes were placed in the PVN bilaterally. The placement of PVN stimulating electrodes was verified histologically after experiments (see 'Histology'). Antidromic activation of MnPO neurones was performed by applying square-wave current pulses (0.5 ms) at a low frequency (0.5–1.0 Hz) with varying amplitude (initially 1.0 mA) to determine threshold intensity. When a neurone displayed a constant onset latency during antidromic stimulation, additional tests were performed to confirm its antidromic nature as described previously (Lipski, 1981). Units were considered to be antidromically activated from the PVN according to the following criteria: (1) displayed a constant latency of the antidromic spike, (2) ability to follow high frequency stimulation (> 250–300 Hz), and (3) collision or cancellation of the stimulus-evoked spike by a spontaneous action potential. For extremely short latency responses (< 5 ms), high frequency stimulation could not always be demonstrated due to interference from the stimulus artifact. Collision of stimulus-evoked spikes by a spontaneous action potential was not performed in a subset of neurones due to a lack of spontaneous activity. All neurones in the present study satisfied at least two criteria.

Physiological stimulation

To selectively stimulate forebrain neurones, solutions of NaCl, mannitol or Ang II were delivered through a catheter advanced into the internal carotid artery (ICA) approximately 1.5–2.0 mm rostral to the carotid bifurcation via the occipital artery. This allows blood flow to be maintained through the carotid arteries while delivering solutions directly to the forebrain. Neuronal responses to hyperosmotic NaCl (0.75 or $1.5\,\mathrm{osmol\,l^{-1}}$), Ang II (150 ng) and isotonic saline ($0.3\,\mathrm{osmol\,l^{-1}}$) delivered to the ICA were examined. In a subset of neurones, hypertonic mannitol ($1.5\,\mathrm{osmol\,l^{-1}}$) was also tested. All solutions were dissolved in isotonic saline and delivered over 10 s in a volume of $100\,\mu$l. Barosensitivity was determined by changes in neuronal discharge to phenylephrine (PE; 4–20 μg kg^{-1}, i.v.) or sodium nitroprusside (SNP; 4–20 μg kg^{-1}, i.v.) to increase or decrease arterial blood pressure, respectively. In some experiments, an inflatable cuff was placed around the descending aorta proximal to the renal vessels to increase ABP non-pharmacologically in the carotid sinus and aortic arch as previously described (Stocker *et al.* 2004).

Unit discharge correlation with sympathetic nerve activity and the cardiac cycle

In some animals, a renal sympathetic nerve was isolated and placed onto a stainless steel wire electrode (A-M system, 0.125 mm O.D.) through a retroperitoneal incision as described previously (Stocker *et al.* 2005). Nerve signals were obtained using a high-impedance probe connected to an AC amplifier equipped with half-amplitude filters (band pass, 30–3000 Hz) and a 60 Hz notch filter. Then, the signal was amplified (10 000–20 000), full-wave rectified and integrated (10 ms time constant) using a moving averager (MA-821RSP, Cwe Inc., Ardmore, PA, USA), and digitized at a frequency of 1000 Hz using a 1401plus analog-to-digital converter and Spike 2 software (Cambridge Electronic Design, Cambridge, UK). Spike-triggered averages were constructed between spontaneous neuronal discharge (> 500 events) and postganglionic renal SNA to determine whether unit discharge exhibited a temporal relationship with renal SNA. These were compared to renal SNA averages constructed from the same number of square-wave pulses delivered randomly at an average frequency approximately equal to the discharge of the recorded neurone. To determine whether spontaneous discharge had a cardiac-cycle-related rhythm, time histograms of unit discharge were constructed and triggered from the R wave of the EKG signal.

Juxtacellular labelling

In a subset of animals ($n = 21$), we attempted to juxtacellularly label the recorded neurone with biotinamide (Molecular Probes, Eugene, OR, USA) or neurobiotin (Vector Laboratories, Burlingame, CA, USA) as described previously (Pinault, 1996). Once neuronal responses were examined in response to the above stimuli, current pulses (200 ms duration, 50% duty cycle) of increasing amplitude (0.5–6 nA) were delivered through the recording electrode containing 5% biotinamide or neurobiotin dissolved in isotonic saline. Once the cell discharge became entrained to the current pulses, the amplitude was adjusted to maintain entrainment without damaging the neurone. These current pulses iontophoretically eject biotinamide to fill the soma and proximal dendrites of the recorded cell.

After 20–120 s of clear entrainment, the current pulses were terminated and the cell was allowed to recover for at least 1 h. Only one entrainment was attempted per experiment.

Histology

At the end of experiments, the recording site was marked by applying DC current through the recording electrode (5 μA, 5 min) if a cell was not entrained. This resulted in a deposit of Chicago Sky Blue or biotinamide in the extracellular space. Stimulating electrodes targeted at the PVN were marked by applying DC current (50 μA, 15 s). Then, the animals were perfused transcardially with 4% paraformaldehyde (4°C, 200 ml) dissolved in 0.1 M PBS. Brains were removed and post-fixed in 4% paraformaldehyde overnight and immersed in 20% sucrose dissolved in 0.1 M PBS for 2–3 days. Brains were sectioned at 50 μm using a sliding microtome. Sections with antidromic stimulation sites were mounted on glass slides, counterstained with cresyl violet, and analysed under a light microscope. All MnPO-PVN neurones in the present study had antidromic stimulation sites located in the middle to caudal third of the PVN and consistently encroached on the posterior magnocellular, dorsal and ventrolateral parvocellular, and/or lateral parvocellular subnuclei. Sections containing juxtacellularly labelled cells (or marked recording sites) were stored in vials containing cryoprotectant (30% sucrose, 30% ethylene glycol, 1% polyvinyl-pyrrolidone in 0.1 M PBS) at −25°C. Labelled cells were visualized by standard immunocytochemical methods. After several rinses in 0.1 M PBS, sections were incubated in a solution containing 0.2% Triton X-100 in 0.1 M PBS plus an avidin–peroxidase conjugate (ABC Vectastain Kit, Vector Laboratories, Burlingame, CA, USA) overnight at 4°C. Sections were then reacted for 4 min in Tris buffer (pH 7.3) containing 0.05% 3,3′-diaminobenzidine tetrahydrochloride (Sigma-Aldrich) and 0.6% hydrogen peroxide. The reaction was terminated with several rinses in 0.1 M PBS. In some experiments, labelled cells were visualized by incubating sections overnight at 4°C with streptavidin–Alexa Fluor 488 (1 : 250, Molecular Probes). All sections were mounted on glass slides, dehydrated in graded alcohols, cleared in xylene, and coverslipped with Cytoseal 60 (Fisher Scientific, Pittsburgh, PA, USA). Recording sites marked with biotinamide were visualized by identical methods.

Retrograde tracing from the PVN

Since there are limited data demonstrating whether MnPO neurones project to the PVN bilaterally, we performed a set of retrograde tracing experiments from both the left and right PVN. Male Sprague-Dawley rats (300–350 g,

$n = 3$) were anaesthetized with 3% isoflurane (in 100% O_2) and placed into a stereotaxic head frame with the skull level between bregma and lambda. After the overlying bone and dura were removed, 4% Fluorogold (10 nl; Fluorochrome, Denver, CO, USA) was microinjected into the PVN as described previously (Stocker *et al.* 2005) using the following coordinates: −1.8 mm caudal to bregma, 0.5–0.7 mm lateral to midline, and 7.65 mm ventral to the dorsal surface of the skull. Rhodamine-labelled fluorescent microspheres (50 nl; LumaFluor, Naples, FL, USA) were microinjected into the contralateral PVN using similar coordinates except the pipette was moved to the opposite side of the brain 0.5–0.7 mm lateral from the midline sinus. All microinjections were performed with glass micropipettes (O.D., 30 μm) connected to a pneumatic picopump (WPI, Sarasota, FL, USA), and the tracers were injected over 30 s. Once the pipette had been left in place for 10 min and removed, the hole in the skull was filled with bone wax, the overlying musculature and skin sutured, and each rat was treated with ampicillin (100 mg kg^{-1}, I.M.) and returned to its home cage.

Approximately 6–8 days later, rats were deeply anaesthetized with urethane (1.5 mg kg^{-1}, I.P.) and perfused transcardially with heparinized isotonic saline (10 units ml^{-1}, 100 ml) followed by 4% paraformaldehyde (4°C, 300 ml) in 0.1 M PBS. Brains were removed, post-fixed overnight in 4% paraformaldehyde, and immersed in 20% sucrose for 2 days. Brains were then sectioned at 30 μm using a sliding microtome, collected into three serially adjacent sets, and stored in vials containing cryoprotectant at −25°C as described above. One set of tissue was rinsed in 0.1 M PBS, mounted on glass slides, and coverslipped using Cytoseal 60 mounting medium (Fisher Scientific, Pittsburgh, PA, USA).

Statistical analysis

Basal discharge of MnPO neurones was determined from a representative 3 min rate-meter record (1 s bins) when ABP was stable. Differences in basal firing rate, antidromic latency, or antidromic threshold were analysed using independent *t* tests (Systat 10.2, Systat Software, Inc., Richmond, CA, USA). Changes in unit discharge in response to hyperosmotic, Ang II and baroreceptor stimulation were analysed by comparing the average 30-s baseline discharge to the average discharge of a 5-s segment after the onset of the stimulus. Values were log-transformed and then statistically analysed using a paired *t* test. To determine whether unit activity was correlated with SNA, spike-triggered averages of renal SNA were compared with averages triggered by the same number of pulses delivered at randomized intervals but with a similar average frequency of the recorded cell discharge. When the amplitude was at least 3-fold greater than the corresponding random

Table 1. Summary of Discharge Characteristics for Type 1-IV MnPO-PVN neurones

Neuronal type	Discharge response	n	Baseline discharge (Hz)	Baroreceptor input (%)	Sympathetic-related discharge (%)	Cardiac-cycle-related rhythm (%)
I – Osmotic	Total	14	1.7 ± 0.9	—	—	—
	↑	11	1.3 ± 1.0	63 (5/8)	33 (1/3)	0 (0/3)
	↓	3	3.4 ± 1.0†	—	50 (1/2)	0 (0/3)
II- Ang II	Total	7	0.7 ± 0.3	—	—	—
	↑	7	0.7 ± 0.3	43 (3/7)	33 (1/3)	0 (0/3)
III – Osmotic + Ang II	Total	16	4.4 ± 1.4*	—	—	—
	↑	14	4.5 ± 1.6	43 (6/14)	45 (5/11)	15 (2/11)
	↓	2	3.6 ± 2.9	0 (0/1)	—	—
IV – Unresponsive	Total	13	0.5 ± 0.4	8 (1/12)	0 (0/6)	0 (0/6)

*Significant difference from type I, II and IV neurones ($P < 0.05$). † Significant difference between discharge responses within a neuronal type ($P < 0.05$). Type I neurones responded to ICA injection of hypertonic NaCl but not Ang II, type II neurones responded to Ang II but not hypertonic NaCl, type III neurones responded to both hypertonic NaCl and Ang II, type IV neurones did not respond to either hypertonic NaCl or Ang II. The direction of the neuronal responses to osmotic or Ang II is indicated under 'Discharge response'. ↑ denotes increase in cell discharge, ↓ denotes decrease in cell discharge. For type III neurones, the direction of the neuronal response was always the same for osmotic and Ang II stimulation. The degree of barosensitivity is presented with each neuronal type. ‡ Baroreceptor inputs were altered by either increasing ABP with an injection of phenylephrine/inflation of an aortic cuff or decreasing ABP with sodium nitroprusside. In all type I, II and III neurones, an increase and decrease in ABP produced a decrease and increase in cell discharge, respectively. Values for baseline discharge are mean ± S.E.M.

pulse-triggered average, unit discharge was considered to possess a significant correlation with renal SNA. To determine whether spontaneous discharge displayed a cardiac cycle-related rhythm, post-EKG R-wave time histograms of unit discharge were constructed. Data for spike-triggered averages and cardiac cycle-related rhythms were taken from a rate-meter record when no stimulus was given. For all comparisons, a P value < 0.05 was considered statistically significant.

For retrograde-labelling experiments, digital images were collected from three rostral–caudal levels of the MnPO (see Fig. 6) using an Olympus IX50 microscope connected to a Spot camera (Spot RT Slider, Diagnostic Instruments, Inc, Sterling Heights, MI, USA) using Spot imaging software (version 3.24). Level 1 was the most rostral and consisted of an incomplete anterior commissure and a small 3rd ventricle. Level 2 displayed a complete anterior commissure that separated the dorsal and ventral MnPO. Level 3 also had a complete anterior commissure but with a compact ventral MnPO and a very prominent 3rd ventricle. Sampling from these three levels represented a section approximately every 100 μm through the rostral–caudal extent of the MnPO. For purposes of visualization, FG and rhodamine-labelled neurones were pseudocoloured green and red, respectively, and images were digitally overlaid. Accordingly, double-labelled neurones appear yellow in the merged images. The number of retrogradely labelled neurones was quantified and compared by an independent t test. When data were expressed as a per cent, groups were compared by a Mann-Whitney U test.

Results

Basal discharge characteristics and antidromic properites

Recordings were made from 65 MnPO neurones with a basal discharge of 2.8 ± 0.5 Hz (range: 0.0–16.7 Hz). Of these units, 50 MnPO neurones were antidromically activated from the PVN with an average onset latency of 11.3 ± 0.7 ms (range: 4–25 ms) and antidromic threshold of 224 ± 20 μA (range: 30–650 μA, 0.5 ms pulse duration). The average conduction velocity was 0.18 ± 0.01 m s^{-1} (range: 0.06–0.45 m s^{-1}) thereby suggesting the axons of these neurones were unmyelinated. Interestingly, only 9.5% (2 of 21) of MnPO-PVN units were antidromically activated from both sides of the PVN, thereby indicating that the majority of MnPO-PVN cells have unilateral projections to the PVN (see 'Retrograde labelling from the PVN'). The basal discharge of MnPO-PVN neurones averaged 2.0 ± 0.5 Hz (range: 0.0–16.7 Hz); 62% (31 of 50) of these cells were spontaneously active with an average discharge of 3.3 ± 0.8 Hz (range: 0.01–16.7 Hz), whereas 38% (19 of 50) were quiescent (basal discharge < 0.01 Hz). The antidromic onset latencies, conduction velocities and antidromic thresholds did not differ between spontaneously active and quiescent MnPO-PVN neurones. However, the majority of quiescent units (63%, 12 of 19) were unresponsive to hyperosmotic, Ang II or baroreceptor stimulation, whereas only 10% (3 of 31) of spontaneously active MnPO-PVN neurones were unresponsive to the same stimuli.

MnPO-PVN neuronal responses to hyperosmotic, Ang II and baroreceptor stimulation

For purposes of presentation, MnPO-PVN neurones were divided into four groups based upon each unit's responses to hyperosmotic and/or Ang II stimulation: (1) type I neurones ($n = 13$) responded to osmotic but not Ang II stimulation; (2) type II neurones ($n = 7$) responded to Ang II but not osmotic stimulation; (3) type III neurones ($n = 16$) responded to both osmotic and Ang II stimulation; and (4) type IV neurones ($n = 14$) did not respond to osmotic or Ang II stimulation. Changes in baroreceptor input produced by increases or decreases

in ABP altered cell discharge in a subset of each neuronal group. Table 1 provides a summary of these discharge characteristics for each neuronal type.

Type I: osmotically responsive MnPO-PVN neurones. ICA injection of 1.5 osmol l^{-1} NaCl significantly increased cell discharge in 79% (11/14) of type I neurones by $624 \pm 135\%$ ($P < 0.01$) and produced a small but significant increase in mean ABP of 12 ± 4 mmHg ($P < 0.05$; baseline mean ABP: 102 ± 4 mmHg). On the other hand, 21% of type I neurones (3/14) showed a significant decrease in firing rate of $-74 \pm 19\%$ after ICA injection of 1.5 osmol l^{-1} NaCl,
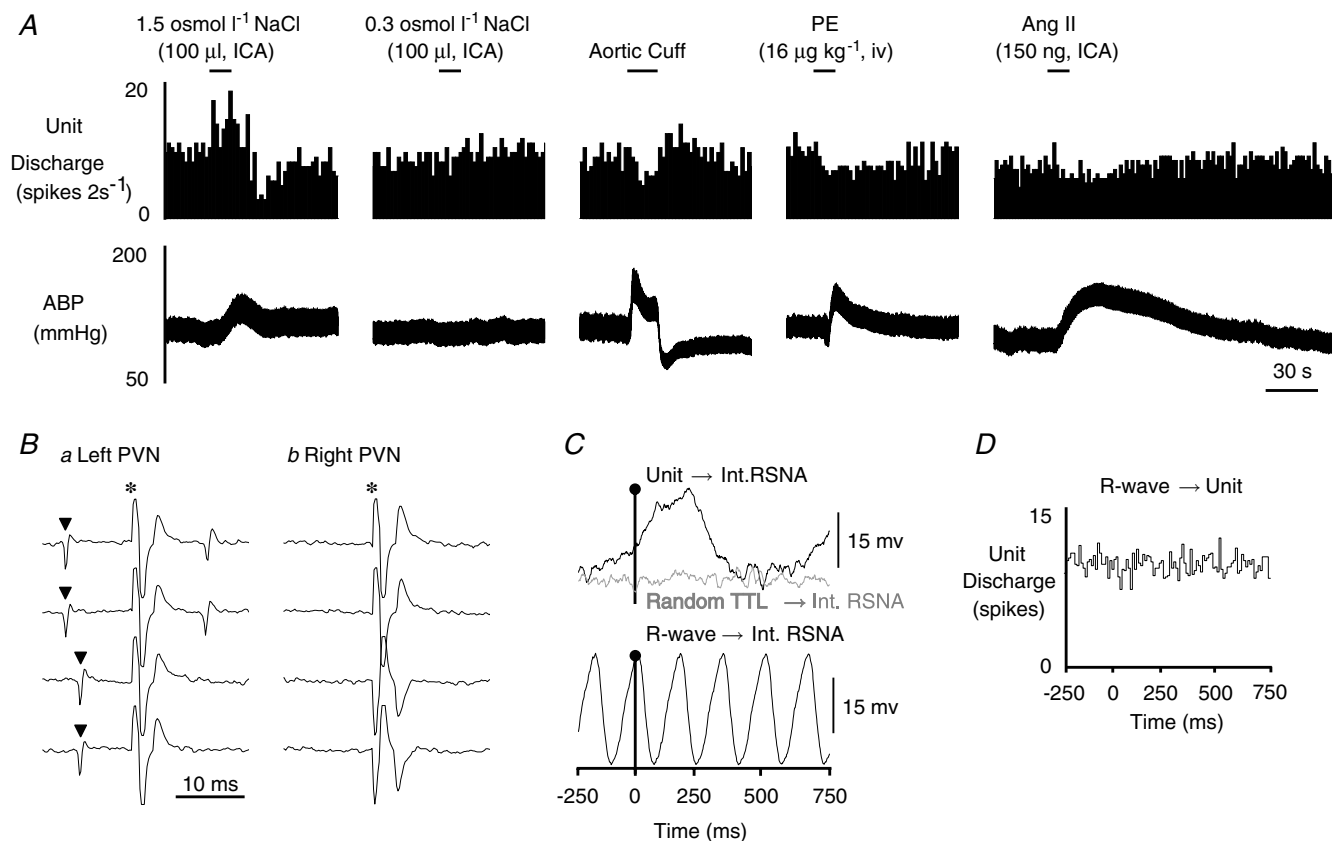

Figure 1. Example of a type I MnPO-PVN neurone

A, ICA injection of hypertonic NaCl but not isotonic saline significantly increased cell discharge. This neurone was also barosensitive as increases in ABP produced by inflation of an aortic cuff or the α-adrenergic agonist phenylephrine (PE) each decreased neuronal firing rate. ICA injection of Ang II slightly but significantly decreased cell discharge. *B*, this neurone was antidromically activated from the left PVN with a constant onset latency of 10 ms and activation threshold of 300 μA (*a*, top two traces). The antidromic spike collided with a spontaneous action potential (*a*, bottom two traces), and the neurone also followed high frequency stimulation (> 333 Hz, trace not shown). In contrast, the neurone could not be antidromically activated with a high stimulus intensity (1 mA, 1 ms) from the contralateral PVN (*b*). *C*, baseline unit discharge positively correlated with renal SNA (RSNA, top trace, peak latency: 240 ms). Note that renal SNA showed no obvious correlation with randomly occurring square-wave pulses (random TTL→ Int RSNA, middle trace) generated at frequencies similar to the spontaneous discharge of the recorded neurone. The bottom trace shows that renal SNA is tightly coupled to the cardiac cycle during the same time as revealed by R-wave-triggered averages of renal SNA. *D*, R-wave-triggered average of unit discharge demonstrates that this MnPO-PVN neurone had no obvious correlation with the cardiac cycle. The spike-triggered averages and histograms presented in *C* and *D* were constructed from 7346 spontaneous unit discharges. ▼, spontaneous action potential; *, stimulus artifact.

and this was associated with a significant increase in mean ABP of 18 ± 1 mmHg ($P < 0.05$; baseline mean ABP 107 ± 5 mmHg). In regard to both neuronal responses, the initial change in cell discharge always preceded the increase in ABP. ICA injection of isotonic saline and/or Ang II had no effect on the cell discharge. A subpopulation of type I neurones were also barosensitive. Approximately 63% (5/8) of these neurones that increased discharge to osmotic stimulation displayed either a decrease in firing rate during an increase in ABP or an increase in cell discharge in response to a decrease in ABP. Figure 1 provides an example of a barosensitive type I MnPO-PVN neurone that increased cell discharge in response to osmotic stimulation but displayed a small but significant decrease in cell discharge after Ang II stimulation. An increase in ABP produced by PE or inflation of an aortic cuff decreased cell discharge. Interestingly, the basal discharge of this type I neurone had a significant and positive correlation with

renal SNA but not with the cardiac cycle (Fig. 1*C* and *D*; Table 1).

Type II: Ang II-responsive MnPO-PVN neurones. ICA injection of Ang II (150 ng) significantly increased cell discharge in 100% (7/7) of type II neurones by $546 \pm 164\%$ ($P < 0.01$), whereas ICA injection of hypertonic NaCl or isotonic saline had no effect. As expected, ICA injection of Ang II significantly increased mean ABP by 38 ± 8 mmHg ($P < 0.01$; baseline mean ABP: 108 ± 4). Figure 2 provides an example of a type II MnPO-PVN neurone that displayed a significant increase in firing rate after ICA injection of Ang II but not after hypertonic or isotonic saline. Interestingly, approximately 43% (3/7) of type II neurones were also barosensitive. In these cells, an increase in ABP consistently decreased cell discharge (Fig. 2*B*). Only one type II neurone had a significant correlation between its basal discharge and renal SNA (Table 1).
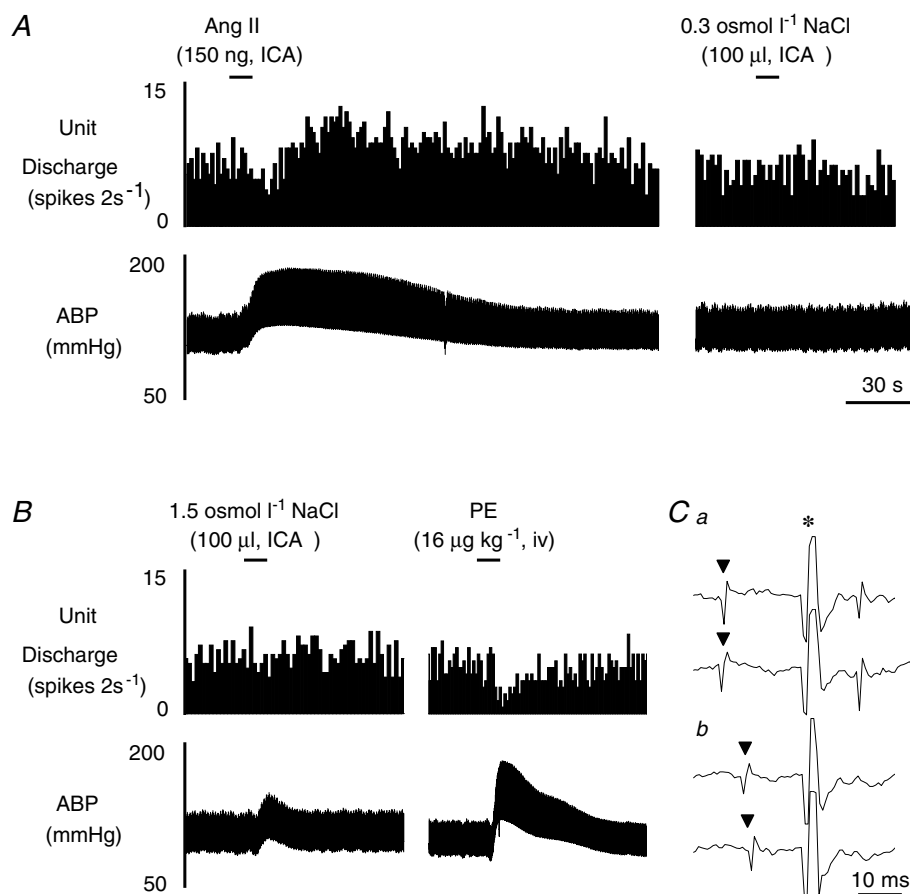

Figure 2. Example of a barosensitive type II MnPO-PVN neurone
A, ICA injection of Ang II significantly increased MnPO-PVN unit discharge whereas isotonic saline had no effect. *B*, ICA injection of hypertonic NaCl did not alter cell discharge; however, baroreceptor activation produced by PE significantly increased ABP but decreased cell discharge. *C*, this MnPO-PVN neurone was antidromically activated from the right PVN (*a*, latency: 12 ms; threshold, 260 μA). The antidromic spike was collided with a spontaneous action potential (*b*). ▼, spontaneous action potential; *, stimulus artifact.

Type III: osmotic and Ang II-responsive MnPO-PVN neurones. A major goal of the present study was to determine whether an individual MnPO-PVN neurone receives both osmotic and peripheral Ang II inputs. ICA injection of both 1.5 osmol l^{-1} NaCl and 150 ng Ang II significantly increased cell discharge in 88% (14/16) of type III neurones by 655 ± 155 and 531 ± 213%, respectively (both $P < 0.01$). These stimuli also produced significant increases in mean ABP of 13 ± 2 mmHg ($P < 0.05$; baseline mean ABP: 104 ± 5 mmHg) and 48 ± 6 mmHg ($P < 0.01$; baseline mean ABP: 106 ± 6 mmHg), respectively. The response magnitude of the change in neuronal discharge or mean ABP for the respective stimulus was not significantly different from those of type I and II neurones. Interestingly, the basal discharge of type III neurones was significantly higher than type I or II neurones (Table 1).

Figure 3 provides an example of a type III neurone that increased cell discharge in response to ICA injection of hypertonic NaCl in a concentration-dependent manner. In addition, ICA injection of Ang II also significantly increased cell discharge. This type III neurone was not barosensitive (Fig. 3B).

As noted above for type I and II neurones, a subpopulation of type III neurones were barosensitive (43%, 6/14). Figure 4 provides an example of a barosensitive type III neurone. ICA injection of hypertonic NaCl concentration-dependently increased cell discharge (Fig. 4A). Hypertonic mannitol also increased cell discharge of this type III neurone. In addition, a decrease in ABP produced a significant increase in cell discharge (Fig. 4A). Interestingly, ICA injection of Ang II produced a biphasic response with an initial decrease in cell discharge as ABP increased followed by a significant
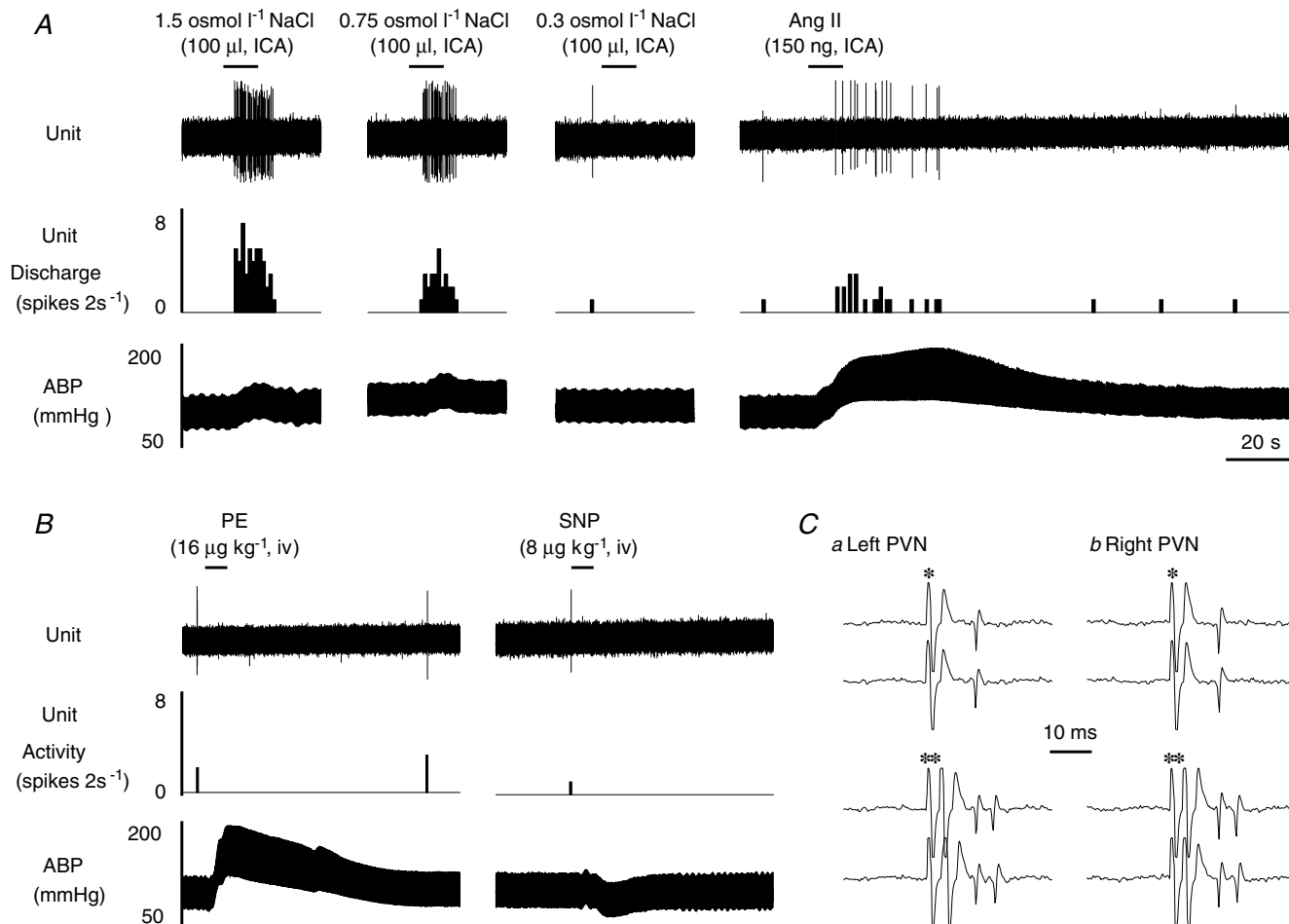

Figure 3. Example of a type III MnPO-PVN neurone
A, ICA injection of hypertonic NaCl concentration-dependently increased MnPO-PVN unit discharge, whereas isotonic saline had no effect. In addition, ICA injection of Ang II significantly increased unit discharge. *B*, the firing rate was unaltered in response to increases or decreases in ABP. *C*, this MnPO-PVN neurone was antidromically activated from the left (*a*, latency: 9 ms; threshold: 200 μA) and right (*b*, latency: 10 ms; threshold: 230 μA) PVN as indicated by the constant latency and ability to follow high frequency stimulation (> 333 Hz). *, stimulus artifact.

increase in neuronal discharge once ABP returned to baseline levels (Fig. 4*B*). This suggests that the increase in ABP may mask any Ang II-evoked increase in discharge of barosensitive type III neurones. To test this hypothesis, we compared the effect of ICA injection of Ang II alone *versus* the effect of ICA injection of Ang II plus co-administration of SNP to prevent the Ang II-evoked increase in ABP in a subset of neurones ($n = 5$). In these cells, ICA injection of Ang II alone significantly increased mean ABP by 45 ± 5 mmHg ($P < 0.001$;
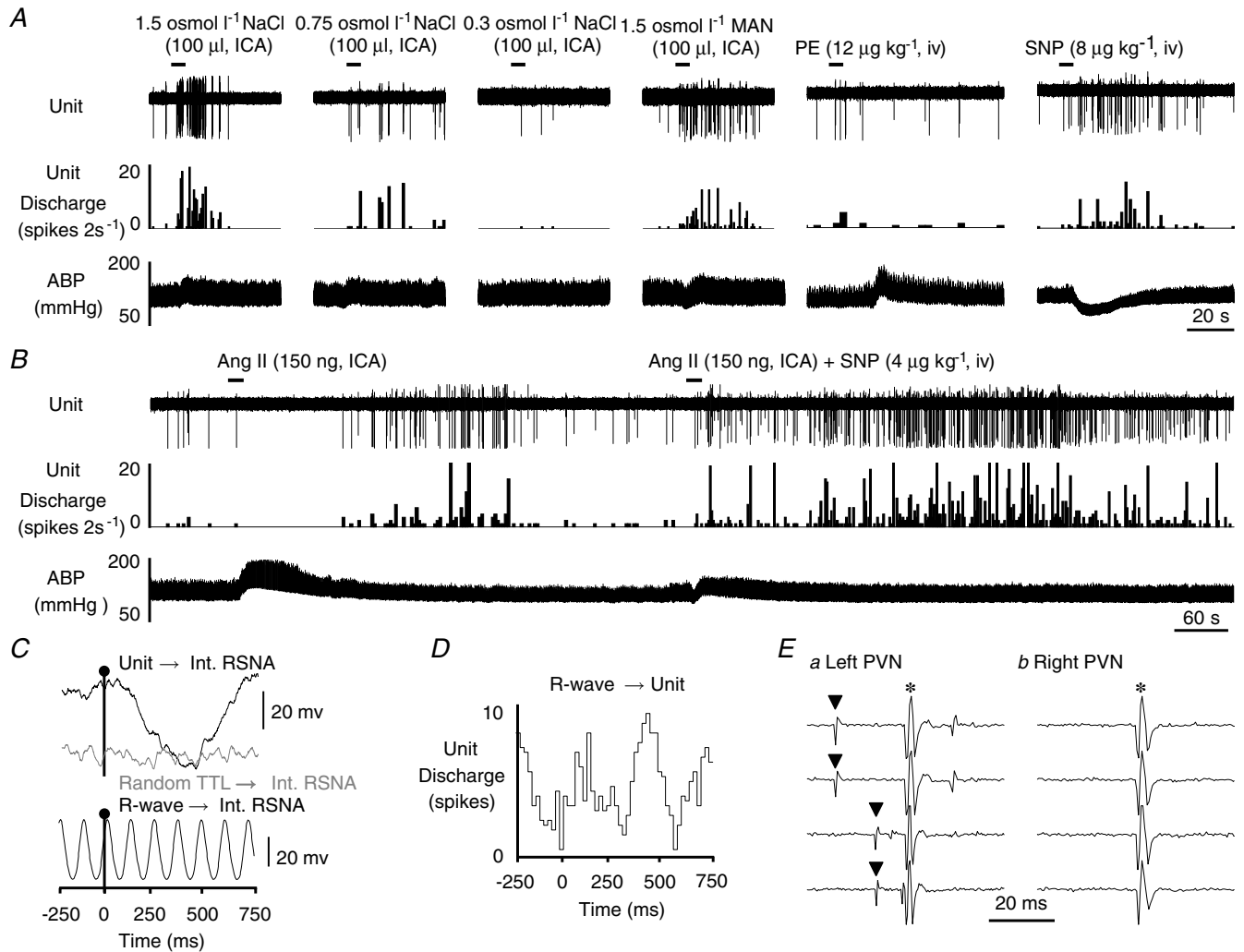

Figure 4. Example of a barosensitive type III MnPO-PVN neurone
A, ICA injection of hypertonic NaCl dose-dependently increased MnPO-PVN cell discharge, whereas isotonic saline had no effect. Hypertonic mannitol (Man) also significantly increased the firing rate of this MnPO-PVN neurone. Moreover, this neurone was barosensitive as SNP decreased ABP and significantly increased cell discharge. *B*, ICA injection of Ang II produced a biphasic response with an initial and significant decrease in discharge rate when ABP was elevated followed by a significant increase in activity once ABP returned to baseline values. When the associated Ang II-evoked increase in ABP was attenuated with SNP, the neurone no longer showed a biphasic response. Instead, Ang II injection evoked an immediate and sustained increased in cell discharge thereby suggesting that the Ang II-evoked increase in ABP was masking the Ang II-excitatory effect on unit activity. *C*, baseline unit discharge significantly correlated with renal SNA (top trace, peak latency: 460 ms) whereas no obvious correlation was observed with randomly occurring square-wave pulses (random TTL→Int. RSNA, middle trace). The bottom trace shows that renal SNA is strongly correlated to the cardiac cycle during the same sampling time as revealed by R-wave-triggered averages of renal SNA. *D*, R-wave-triggered time histogram average of unit discharge showed a significant cardiac-cycle-related rhythm. The spike-triggered averages and histograms presented in *C* and *D* were constructed from 1366 spontaneous unit discharges. *E*, the neurone was antidromically activated from the left PVN with a constant onset latency of 14 ms and threshold of 130 μA (*a*, top two traces), followed high frequency stimulation (traces not shown), and the antidromic spike was collided with a spontaneous action potential (*a*, bottom two traces). In contrast, the same neurone could not be antidromically activated with a high stimulus intensity (1 mA, 1 ms) from the contralateral PVN (*b*). ▼, spontaneous action potential; *, stimulus artifact.

baseline: 109 ± 7 mmHg *versus* peak: 155 ± 9 mmHg), but this was associated with an initial and significant decrease in cell discharge by $45 \pm 19\%$ ($P < 0.05$). When SNP was administered with ICA injection of Ang II, the Ang II-evoked increase in ABP was significantly attenuated as MAP rose only 16 ± 5 mmHg (baseline: 108 ± 8 mmHg *versus* peak: 124 ± 7 mmHg, $P < 0.05$). However, this was associated with a significant increase, rather than decrease, in cell discharge by $556 \pm 167\%$ (baseline: 1.7 ± 1.0 Hz *versus* peak: 5.0 ± 3.3 Hz, $P < 0.01$). Figure 4*B* illustrates this effect on a type III neurone.

Interestingly, 45% (5/11) of type III neurones displayed a significant correlation with renal SNA (Table 1) – three

neurones had a positive peak whereas two neurones had a negative peak (Fig. 4*C*). Only 15% of type III neurones displayed a significant cardiac cycle-related rhythm (Fig. 4*D*, Table 1). The presence of sympathetic-related discharge (positive or negative) or cardiac-cycle-related rhythm was present in type III neurones that displayed an increase in cell discharge to osmotic and Ang II stimulation.

Only 12% (2/16) of type III neurones displayed a decrease in firing rate in response to both hypertonic NaCl and Ang II. Again, both treatments significantly increased mean ABP by 11 ± 4 mmHg ($P < 0.05$; baseline mean ABP: 115 ± 6 mmHg) and 46 ± 4 mmHg ($P < 0.01$;
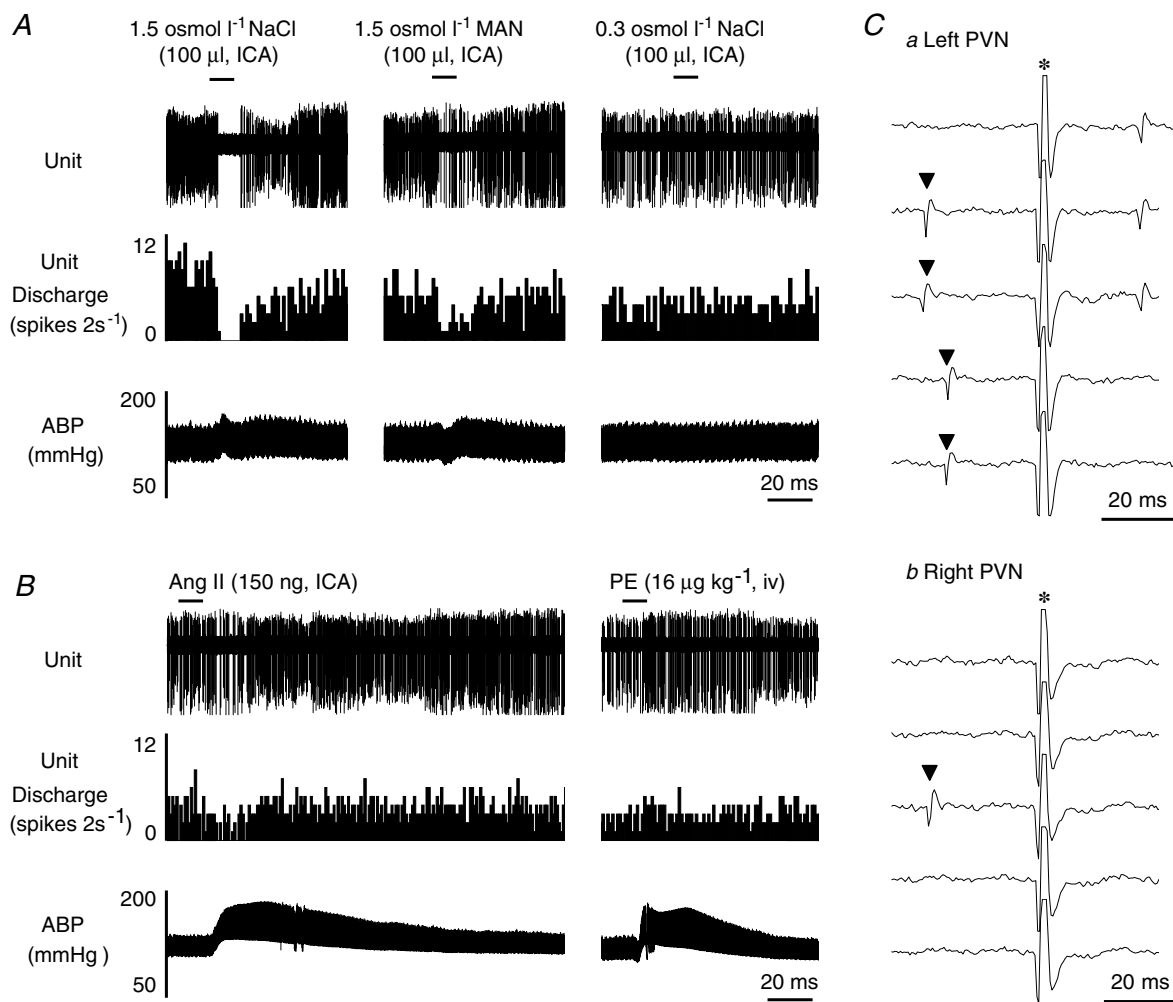

Figure 5. Example of a type III MnPO-PVN neurone that displayed a decrease in cell discharge in response to osmotic and Ang II stimulation

A, ICA injection of hypertonic NaCl and mannitol significantly decreased MnPO cell discharge whereas isotonic saline had no effect. *B*, ICA injection of Ang II also decreased cell discharge whereas baroreceptor activation by a PE-evoked increase in ABP had no effect on the firing rate of this MnPO-PVN neurone. *Ca*, this neurone was antidromically activated from the left PVN with a constant latency (25 ms) and small stimulus threshold (190 μA, top three traces) and followed high-frequency stimulation (> 333 Hz, traces not shown). Moreover, the antidromic spike was collided with a spontaneous action potential (bottom two traces). *Cb*, again, this unit could not be antidromically activated from the contralateral PVN (1 mA, 1 ms). ▼, spontaneous action potential; *, stimulus artifact.

baseline mean ABP: 115 ± 8 mmHg), respectively. The magnitude of the change in mean ABP was not different from those values when neuronal discharge increased. Figure 5 provides an example of a type III neurone that displayed a significant decrease in cell discharge in response to ICA injection of hypertonic saline or mannitol and ICA injection of Ang II.

Type IV: unresponsive MnPO-PVN neurones. ICA injection of hypertonic NaCl and Ang II failed to significantly alter cell discharge in 13 type IV neurones (Table 1). The changes in mean ABP during osmotic and Ang II stimulation were not different from those reported for type I, II and III neurones. However, one type IV neurone was barosensitive but increased cell discharge in response to an increase in ABP produced by a bolus injection of PE or inflation of an aortic cuff (trace not shown).

Location and juxtacellular labelling of MnPO-PVN neurones

Figure 6 is a schematic of three rostral–caudal levels of the MnPO illustrating the location of type I, II and III MnPO-PVN neurones. Responsive units were located throughout the rostral–caudal and dorsal–ventral extent of the MnPO. In a subset of MnPO-PVN neurones, we attempted to fill these units with biotinamide by juxtacellular labelling as described

elsewhere (Pinault, 1996). Figure 7*A* illustrates the typical steps in the juxtacellular-labelling procedure. Initially, the cell discharge is not entrained to 'simulated' current pulses (200 ms, 50% duty cycle). After increasing the stimulus intensity of current pulses delivered through the recording electrode, the unit activity becomes strongly entrained to the current pulses. Once the current pulses are terminated, the cell recovers and its activity is no longer entrained to the 'simulated' current pulses. Successful labelling was obtained in 86% (18/21) of MnPO-PVN neurones, and these cells were located in either the ventral ($n = 11$, Fig. 7*B*) or dorsal ($n = 7$, Fig. 7*C*) MnPO. These neurones typically had a small soma ($< 25 \mu$m) with one or two primary dendrites that extended into the middle of the MnPO. Presumptive axons of MnPO-PVN neurones coursed caudally to the PVN along the wall of the 3rd ventricle.

Retrograde labelling from the PVN

Since antidromic activation of MnPO units from the PVN suggested that less than 10% of MnPO-PVN neurones have a bilateral projection to the PVN, we sought to confirm this observation by microinjecting two different retrograde tracers into opposite sides of the PVN and quantifying the number of retrogradely labelled MnPO neurones. Microinjection of fluorogold and rhodamine-labelled microspheres into the PVN produced a similar number of retrogradely labelled neurones in the MnPO (fluorogold:
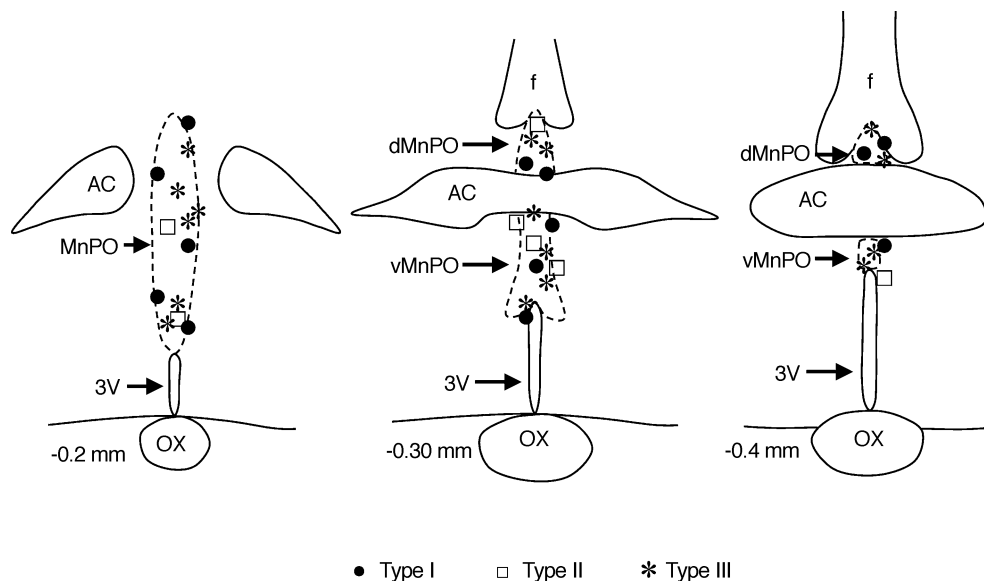

● Type I   □ Type II   ✳ Type III

Figure 6. Location of type I, II and III MnPO-PVN neurones
Type I, II and III MnPO-PVN neurones were located throughout the rostral–caudal and dorsal–ventral extent of the MnPO. The location of non-responsive neurones was similar (sites not shown). Coordinates are in reference to bregma using standard sections from the atlas of Paxinos and Watson (Paxinos & Watson, 1998). dMnPO, dorsal median preoptic nucleus; vMnPO, ventral median preoptic nucleus; AC, anterior commissure; f, fornix; 3V, 3rd ventricle; OX, optic chiasm.

327 ± 34 neurones *versus* rhodamine: 279 ± 37 neurones; Fig. 8); however, very few neurones contained both tracers (11 ± 4 neurones; Fig. 8). When expressed as a percentage, only $3.3 \pm 1.0\%$ of fluorogold-positive neurones contained rhodamine microspheres, whereas $3.8 \pm 1.0\%$ of rhodamine-positive neurones contained fluorogold. Interestingly, the distribution of labelled neurones in the MnPO was not limited to the ipsilateral side of the injection; rather, cells were spread throughout the nucleus. Similar to the MnPO, less than 10% of neurones in the subfornical organ and the organum vasculosum of the lamina terminalis were positive for both fluorogold and rhodamine-labelled microspheres (data not shown).

Discussion

Previous studies have demonstrated that the MnPO plays a pivotal role in the autonomic, neuroendocrine and/or behavioural responses to hyperosmolality, elevated circulating Ang II levels and changes in arterial blood

pressure/blood volume (Johnson & Loewy, 1990; Johnson *et al.* 1996). Despite the potential integrative role of the MnPO, it is not known whether osmotic, circulating Ang II and baroreceptor inputs target identical or distinct populations of MnPO-PVN neurones. The present study provides several new key observations: (1) ICA injection of Ang II increased the discharge of MnPO-PVN neurones (type II); (2) baroreceptor inputs altered the discharge of osmotically and/or Ang II-responsive MnPO-PVN neurones (type I, II and III); (3) individual MnPO-PVN neurones (type III) displayed an increase in cell discharge in response to both osmotic and peripheral Ang II stimulation; (4) a subset of responsive MnPO-PVN neurones (type I, II and III) display sympathetic- and/or cardiac-cycle-related discharge; and (5) both electro-physiological and anatomical data demonstrate that the majority of MnPO-PVN neurones have a unilateral projection to the PVN.

Elevated plasma Ang II levels stimulate the ingestion of water (Fitzsimons, 1998), secretion of vasopressin and oxytocin (Iovino & Steardo, 1984; Stocker *et al.* 2004),
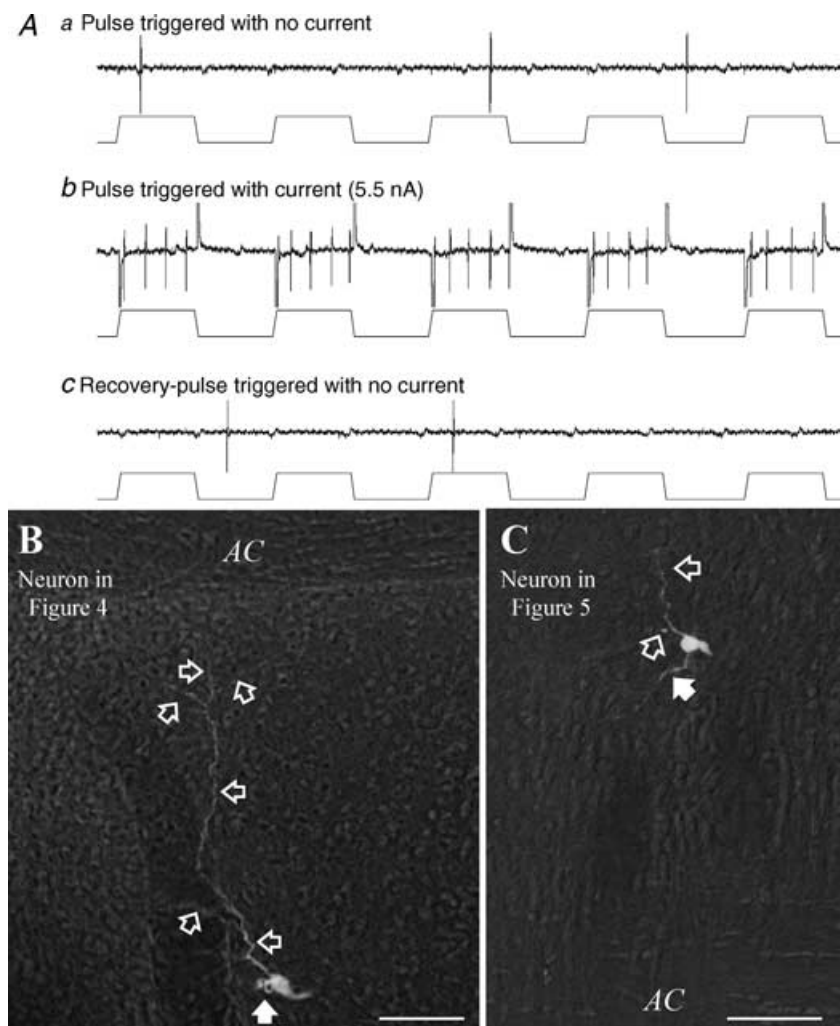

Figure 7. Juxtacellular labelling of MnPO-PVN neurones

Aa, the resting discharge of a MnPO-PVN neurone responsive to osmotic, Ang II and baroreceptor stimulation presented in Fig. 4 was not entrained to the 'simulated' current steps. *Ab*, after increasing stimulus intensity, the discharge of the recorded neurone was entrained to the current pulses for 110 s. *Ac*, once the current pulses were terminated, the original discharge rate returned and was no longer entrained to the 'simulated' current pulses. *B*, the neurone was located in the ventral MnPO at the level of the anterior commissure. Note the extension of dendrites toward the anterior commissure and into the MnPO (open arrows), whereas the axon (filled arrow) coursed along the third ventricle to the PVN. *C*, another example of a MnPO-PVN neurone presented in Fig. 5 that was entrained for 35 s with 2 nA and located in the dorsal MnPO. Scal bar, 50 μm. AC, anterior commissure.

and Fos immunoreactivity in forebrain lamina terminalis structures including the MnPO (Oldfield *et al.* 1994; Potts *et al.* 1999). Lesions of the MnPO attenuate the increase in water intake and vasopressin secretion during increases in plasma Ang II levels (Mangiapane *et al.* 1983; Cunningham *et al.* 1991, 1992), but whether circulating Ang II increases the discharge of MnPO neurones was not known previously. In the present study, we clearly demonstrate that ICA injection of Ang II significantly increased the discharge of MnPO-PVN neurones (type II and III). Interestingly, a subset of these type II and III neurones were barosensitive, and the Ang II-evoked pressor response appeared to mask the Ang II-evoked increase in cell discharge. That is, attenuation of the increase in ABP during ICA Ang II application resulted in a significantly greater increase in MnPO-PVN neuronal discharge. In an analogous manner, Potts and colleagues (Potts *et al.* 1999) have reported that i.v. infusion of Ang II produces a significantly greater level of Fos immuno-

reactivity in forebrain structures including the MnPO in barodenervated *versus* barointact rabbits. The functional significance for this effect may be that the responsiveness of MnPO neurones to neurohumoral stimuli depends on the prevailing levels of ABP and/or blood volume. Consistent with this notion, several investigators have postulated that the pressor action of exogenously administered Ang II may mask the ability of Ang II to stimulate vasopressin secretion and/or thirst (Mitchell *et al.* 1982; Robinson & Evered, 1987; Schreihofer *et al.* 2000; Stocker *et al.* 2001, 2002, 2004). Although barodenervation or attenuation of the peripheral Ang II-evoked pressor response does not further enhance plasma levels of vasopressin and oxytocin (Schreihofer *et al.* 2000; Stocker *et al.* 2004), barodenervation or prevention of the Ang II-pressor response does enhance thirst (Robinson & Evered, 1987; Schreihofer *et al.* 2000; Stocker *et al.* 2001, 2002) and acutely increases sympathetic outflow (Xu & Sved, 2002) during an i.v. infusion of Ang II. Whether either of these
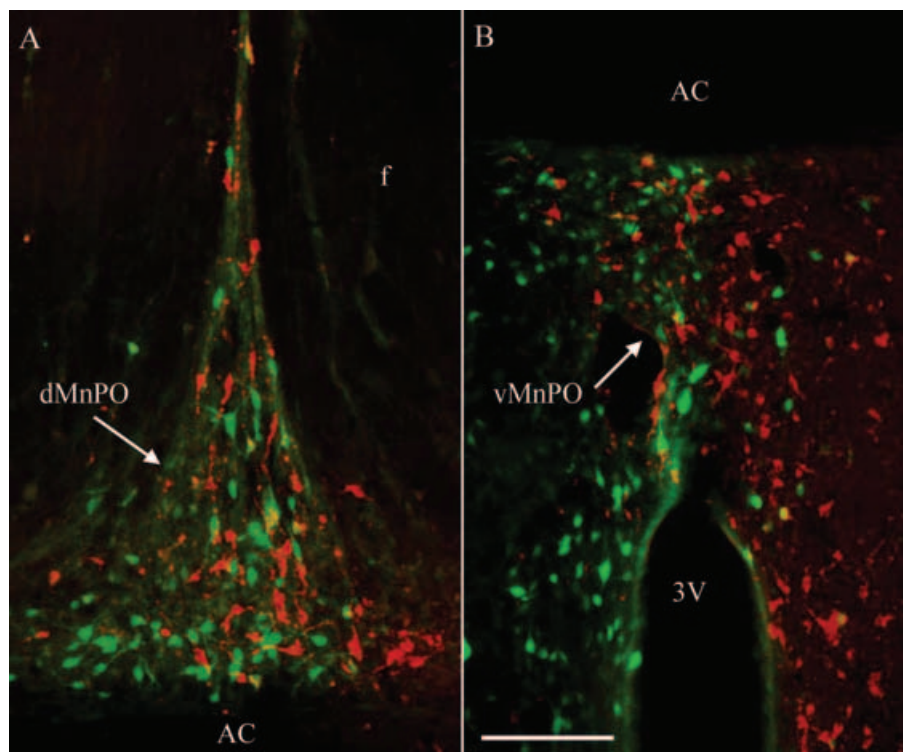

Figure 8. Example of retrogradely labelled neurones in the MnPO after microinjection of fluorogold and rhodamine-labelled microspheres into separate sides of the PVN
Fluorogold-positive neurones are green, neurones with rhodamine-labelled microspheres are red, and neurones that co-localize fluorogold and rhodamine microspheres are yellow. Retrogradely labelled neurones from the PVN were present in both the dorsal (*A*) and ventral (*B*) MnPO as well as the precommissural MnPO. The number of retrogradely labelled neurones was not significantly different between retrograde tracers. Moreover, only $3.3 \pm 1.0\%$ and $3.8 \pm 1.0\%$ of fluorogold- and rhodamine-positive neurones, respectively, co-localized with the second retrograde tracer, thereby indicating that the majority of MnPO neurones have a unilateral projection to the PVN. Scal bar, 100 μm. dMnPO, dorsal median preoptic nucleus; vMnPO, ventral median preoptic nucleus; AC, anterior commissure; f, fornix; 3V, 3rd ventricle.

responses depends on the integration of circulating Ang II levels and baroreceptor inputs by MnPO-PVN neurones awaits further investigation.

Hyperosmolality also stimulates the ingestion of water, secretion of vasopressin and oxytocin, and changes in sympathetic outflow (Bourque *et al.* 1994; Weiss *et al.* 1996; Chen & Toney, 2001). To the extent that it has been investigated, lesion or inactivation of the MnPO attenuates each of the aforementioned responses (Mangiapane *et al.* 1983; Gardiner & Stricker, 1985; Gardiner *et al.* 1985; Cunningham *et al.* 1991, 1992; Yasuda *et al.* 2000). Consistent with these findings, previous studies have reported that hyperosmolality increases the discharge of MnPO neurones (McAllen *et al.* 1990; Tanaka *et al.* 1995; Aradachi *et al.* 1996). Our findings confirm and extend these observations as ICA injection of hypertonic NaCl and mannitol concentration-dependently increased the discharge of MnPO-PVN neurones (type I and III). Moreover, some of these type I and III neurones were barosensitive. The possible convergence of osmotic and baroreceptor inputs onto MnPO-PVN neurones probably has functional significance as an increase in ABP has been reported to inhibit thirst stimulated by hyperosmolality (Stocker *et al.* 2001, 2002). Moreover, barodenervation results in a greater sympthoexcitatory response to ICA injection or i.v. infusion of hypertonic NaCl (Weiss *et al.* 1996; Chen & Toney, 2001). Future studies are needed to determine whether these responses (e.g. thirst, sympathetic outflow) depend upon synaptic integration within MnPO and/or at downstream targets. The neural pathways and cellular mechanisms by which baroreceptor information is transmitted to MnPO neurones remains largely unexplored; however, the MnPO has afferent connections with catecholaminergic and non-catecholaminergic neurones in the nucleus tractus solitarius and ventrolateral medulla (Saper *et al.* 1983) – two areas known to contain neurones responsive to changes in ABP.

As noted above, lesion or inactivation of the MnPO disrupts drinking behaviour, neurohypophyseal secretion of vasopressin, and centrally mediated pressor responses stimulated by hyperosmolaity and Ang II (Mangiapane *et al.* 1983; Gardiner & Stricker, 1985; O'Neill & Brody, 1987; Cunningham *et al.* 1991, 1992; Yasuda *et al.* 2000). Although a myriad of studies have reported that each stimulus increases Fos immunoreactivity in the MnPO (Oldfield *et al.* 1994; Potts *et al.* 1999), such studies are limited as they cannot reveal whether a single neurone responds to a number of different stimuli. In the present study, we demonstrate that ICA injection of both hypertonic NaCl and Ang II increased cell discharge in a number of MnPO-PVN neurones (type III). Moreover, a subset of these neurones was barosensitive. These observations strongly suggest the MnPO may serve as a forebrain integration site for both humoral and visceral

afferent information related to body fluid homeostasis and autonomic function.

Since a subset of osmotic- and/or Ang II-responsive MnPO-PVN neurones was barosensitive, this raises the possibility that the increase in ABP associated with osmotic and/or Ang II stimulation may influence the change in cell discharge. Indeed, we directly explored this possibility and observed such an effect in a subset of Ang II-responsive MnPO-PVN neurones (type II and III). With regard to osmotically responsive MnPO-PVN neurones, the initial increase in cell discharge consistently preceded the increase in ABP during ICA injection of hypertonic NaCl. Thus, at least a portion of the osmotically evoked change in cell discharge is not likely to be influenced by ABP. Since we did not consistently clamp ABP at baseline levels during osmotic or Ang II stimulation, the absolute number of osmotic- and Ang II-responsive neurones may be underestimated, and the relative number of type I, II and III MnPO-PVN neurones may not reflect the true response characteristics. However, the present findings do, in fact, provide clear evidence that individual MnPO-PVN neurones are responsive to multiple neurohumoral stimuli including osmotic, circulating Ang II and baroreceptor input.

Several investigators have reported retrograde labelling of MnPO neurones following injection of transneuronal pseudorabies virus into sympathetically innervated organs such as the kidney or sympathetic ganglia (Westerhaus & Loewy, 1999; Sly *et al.* 2001; Cano *et al.* 2004). In the present study, we found populations of type I, II and III MnPO-PVN neurones that displayed a basal discharge that significantly correlated with renal SNA. Interestingly, every MnPO-PVN neurone with sympathetic-related discharge responded to osmotic and/or Ang II stimulation. However, such a correlation does not prove these MnPO-PVN neurones are functionally linked to the control of SNA. Whether these neurones represent a distinct population of cells that participate in appropriate cardiovascular and autonomic responses during elevations in plasma osmolality and circulating Ang II levels remains to be fully explored.

Anatomical studies have demonstrated that MnPO neurones densely innervate magnocellular and parvocellular neurones of the PVN (Sawchenko & Swanson, 1983; Zardetto-Smith *et al.* 1993). Our present findings extend those observations as electrophysiological experiments demonstrate that the majority of MnPO-PVN neurones were antidromically activated unilaterally from the PVN. In agreement, our anatomical findings with retrograde tracers microinjected into the left and right PVN suggest less than 10% of MnPO-PVN neurones project to the PVN bilaterally. Similar observations have been made with MnPO neuronal projections to the supraoptic nuclei (Renaud *et al.* 1993). Interestingly, Weiss & Hatton (1990) reported that only a few MnPO neurones

project to both the PVN and supraoptic nucleus. This raises the possibility that the MnPO contains different populations of neurones – those controlling neurohypophysial secretion *versus* autonomic outflow *versus* ingestive behaviour. While we did not investigate the neurochemical phenotype of these MnPO-PVN neurones, previous immunocytochemical and *in situ* hybridization studies have reported MnPO neurones contain a number of neurotransmitters/neurotransmitter markers including neurotensin, met-enkephalin, substance P, GABA (GAD65 and GAD67 mRNA), and glutamate (vesicular glutamate transporter-2 mRNA) (Moga & Saper, 1994; Westerhaus *et al.* 1999; Grob *et al.* 2003; Lin *et al.* 2003). Given the neurochemical complexity of MnPO neurones, it would be interesting to speculate that functional inputs target neurochemically distinct populations of MnPO neurones or those MnPO-PVN neurones with a sympathetic-related discharge are neurochemically distinct.

Synaptic integration within the MnPO

The forebrain lamina terminalis contains several interconnected structures along the rostral wall of the third ventricle that include the MnPO and two circumventricular organs: the organum vasculosum of the lamina terminalis and the subfornical organ. In general, the latter two structures sense or detect changes in plasma osmolality and circulating Ang II levels, respectively (Johnson & Loewy, 1990; Johnson *et al.* 1996); however, it is noteworthy that these structures probably contain some neurones responsive to either stimulus (Gutman *et al.* 1988; Oldfield *et al.* 1994). While lesions of the subfornical organ and organum vasculosum of the lamina terminalis significantly attenuate the ingestion of water and secretion of vasopressin to circulating Ang II levels and hyperosmolality, respectively (Johnson & Loewy, 1990; Johnson *et al.* 1996), lesions of the MnPO attenuate these responses to both stimuli (Mangiapane *et al.* 1983; Gardiner & Stricker, 1985; Gardiner *et al.* 1985; Cunningham *et al.* 1991, 1992). These observations together with the dense innervation of the MnPO by neurones in these two circumventricular structures raises the possibility that the MnPO serves as the integration site for these neurohumoral signals. The present electrophysiological data strongly support this notion as hyperosmotic and circulating Ang II inputs targeted overlapping populations of MnPO-PVN neurones. However, the present data do not directly address whether these neurohumoral inputs independently 'converge' onto MnPO neurones or whether MnPO-PVN neurones receive an integrated signal.

Despite the abundance of evidence provided by functional studies to support an integrative role for the MnPO, relatively little is known regarding the synaptic mechanisms by which these neurohumoral stimuli

mediate changes in neuronal excitability. Anatomical studies suggest a small proportion of subfornical organ neurones that project to the MnPO are immunoreactive for Ang II (Lind *et al.* 1984). A functional role for Ang II as a neurotransmitter in the subfornical organ–MnPO pathway is supported by *in vivo* electrophysiological evidence as iontophoretic blockade of Ang II receptors attenuated the increase in MnPO neuronal discharge during electrical stimulation of subfornical organ (Tanaka *et al.* 1986, 1987). This is consistent with *in vitro* patch-clamp studies demonstrating that Ang II depolarizes MnPO neurones by activation of Ang II type 1A receptors (Bai & Renaud, 1998). On the other hand, recent *in vitro* evidence suggests that both $GABA_A$ and glutamatergic ionotropic receptors mediate fast neurotransmission from the subfornical organ to the MnPO (Kolaj *et al.* 2004). In contrast, much less is known regarding the neurochemical inputs originating from the organum vasculosum of the lamina terminalis; however, *in situ* hybridization studies suggest that this region contains the vesicular glutamate transporter-2 (Lin *et al.* 2003) and activation of glutamatergic receptors has been postulated to mediate inputs from organum vasculosum of the lamina terminalis onto supraoptic magnocellular neurones (Bourque & Richard, 2001). Insight into the synaptic and cellular mechanisms by which neurohumoral inputs lead to changes in neuronal excitability may identify distinct populations of MnPO neurones that are anatomically and/or functionally linked to neuroendocrine, behavioural and autonomic responses relevant to body fluid homeostasis and cardiovascular regulation.

References

Aradachi H, Honda K, Negoro H & Kubota T (1996). Median preoptic neurones projecting to the supraoptic nucleus are sensitive to haemodynamic changes as well as to rise in plasma osmolality in rats. *J Neuroendocrin* **8**, 35–43.

Bai D & Renaud LP (1998). ANG II AT1 receptors induce depolarization and inward current in rat median preoptic neurons in vitro. *Am J Physiol Regul Integr Comp Physiol* **275**, R632–R639.

Bourque CW, Oliet SH & Richard D (1994). Osmoreceptors, osmoreception, and osmoregulation. *Front Neuroendocrinol* **15**, 231–274.

Bourque CW & Richard D (2001). Axonal projections from the organum vasculosum lamina terminalis to the supraoptic nucleus: functional analysis and presynaptic modulation. *Clin Exp Pharm Physiol* **28**, 570–574.

Cano G, Card JP & Sved AF (2004). Dual viral transneuronal tracing of central autonomic circuits involved in the innervation of the two kidneys in rat. *J Comp Neurol* **471**, 462–481.

Chen QH & Toney GM (2001). AT(1)-receptor blockade in the hypothalamic PVN reduces central hyperosmolality-induced renal sympathoexcitation. *Am J Physiol Regul Integr Comp Physiol* **281**, R1844–R1853.

Cunningham JT, Beltz T, Johnson RF & Johnson AK (1992). The effects of ibotenate lesions of the median preoptic nucleus on experimentally-induced and circadian drinking behavior in rats. *Brain Res* **580**, 325–330.

Cunningham JT, Sullivan MJ, Edwards GL, Farinpour R, Beltz TG & Johnson AK (1991). Dissociation of experimentally induced drinking behavior by ibotenate injection into the median preoptic nucleus. *Brain Res* **554**, 153–158.

Fitzsimons JT (1998). Angiotensin, thirst, and sodium appetite. *Physiol Rev* **78**, 583–686.

Gardiner TW & Stricker EM (1985). Impaired drinking responses of rats with lesions of nucleus medianus: circadian dependence. *Am J Physiol Regul Integr Comp Physiol* **248**, R224–R230.

Gardiner TW, Verbalis JG & Stricker EM (1985). Impaired secretion of vasopressin and oxytocin in rats after lesions of nucleus medianus. *Am J Physiol Regul Integr Comp Physiol* **249**, R681–R688.

Grob M, Trottier JF, Drolet G & Mouginot D (2003). Characterization of the neurochemical content of neuronal populations of the lamina terminalis activated by acute hydromineral challenge. *Neurosci* **122**, 247–257.

Gutman MB, Ciriello J & Mogenson GJ (1988). Effects of plasma angiotensin II and hypernatremia on subfornical organ neurons. *Am J Physiol Regul Integr Comp Physiol* **254**, R746–R754.

Iovino M & Steardo L (1984). Vasopressin release to central and peripheral angiotensin II in rats with lesions of the subfornical organ. *Brain Res* **322**, 365–368.

Johnson AK, Cunningham JT & Thunhorst RL (1996). Integrative role of the lamina terminalis in the regulation of cardiovascular and body fluid homeostasis. *Clin Exp Pharm Physiol* **23**, 183–191.

Johnson AK & Loewy AD (1990). Circumventricular organs and their role in visceral functions. In *Central Regulation of Autonomic Function*, ed. Loewy AD & Spyer KM, pp. 247–267. Oxford University Press, New York.

Kolaj M, Bai D & Renaud LP (2004). GABAB receptor modulation of rapid inhibitory and excitatory neurotransmission from subfornical organ and other afferents to median preoptic nucleus neurons. *J Neurophysiol* **92**, 111–122.

Lin W, McKinney K, Liu L, Lakhlani S & Jennes L (2003). Distribution of vesicular glutamate transporter-2 messenger ribonucleic acid and protein in the septum-hypothalamus of the rat. *Endocrinology* **144**, 662–670.

Lind RW, Swanson LW & Ganten D (1984). Angiotensin II immunoreactivity in the neural afferents and efferents of the subfornical organ of the rat. *Brain Res* **321**, 209–215.

Lipski J (1981). Antidromic activation of neurones as an analytic tool in the study of the central nervous system. *J Neurosci Meth* **4**, 1–32.

McAllen RM, Pennington GL & McKinley MJ (1990). Osmoresponsive units in sheep median preoptic nucleus. *Am J Physiol Regul Integr Comp Physiol* **259**, R593–R600.

Mangiapane ML, Thrasher TN, Keil LC, Simpson JB & Ganong WF (1983). Deficits in drinking and vasopressin secretion after lesions of the nucleus medianus. *Neuroendocrinology* **37**, 73–77.

Mitchell LD, Barron K, Brody MJ & Johnson AK (1982). Two possible actions for circulating angiotensin II in the control of vasopressin release. *Peptides* **3**, 503–507.

Moga MM & Saper CB (1994). Neuropeptide-immunoreactive neurons projecting to the paraventricular hypothalamic nucleus in the rat. *J Comp Neurol* **346**, 137–150.

Oldfield BJ, Badoer E, Hards DK & McKinley MJ (1994). Fos production in retrogradely labelled neurons of the lamina terminalis following intravenous infusion of either hypertonic saline or angiotensin II. *Neurosci* **60**, 255–262.

Oldfield BJ, Miselis RR & McKinley MJ (1991). Median preoptic nucleus projections to vasopressin-containing neurones of the supraoptic nucleus in sheep. A light and electron microscopic study. *Brain Res* **542**, 193–200.

O'Neill TP & Brody MJ (1987). Role for the median preoptic nucleus in centrally evoked pressor responses. *Am J Physiol Regul Integr Comp Physiol* **252**, Part 2, R1165–R1172.

Paxinos G & Watson C (1998). *The Rat Brain in Stereotaxic Coordinates, CD-Rom*. Academic Press, San Diego.

Pinault D (1996). A novel single-cell staining procedure performed in vivo under electrophysiological control: morpho-functional features of juxtacellularly labeled thalamic cells and other central neurons with biocytin or Neurobiotin. *J Neurosci Meth* **65**, 113–136.

Potts PD, Hirooka Y & Dampney RA (1999). Activation of brain neurons by circulating angiotensin II: direct effects and baroreceptor-mediated secondary effects. *Neurosci* **90**, 581–594.

Renaud LP, Cunningham JT, Nissen R & Yang CR (1993). Electrophysiology of central pathways controlling release of neurohypophysial hormones. Focus on the lamina terminalis and diagonal band inputs to the supraoptic nucleus. *Ann N Y Acad Sci* **689**, 122–132.

Robinson MM & Evered MD (1987). Pressor action of intravenous angiotensin II reduces drinking response in rats. *Am J Physiol Regul Integr Comp Physiol* **252**, R754–R759.

Saper CB, Reis DJ & Joh T (1983). Medullary catecholamine inputs to the anteroventral third ventricular cardiovascular regulatory region in the rat. *Neuroscience Lett* **42**, 285–291.

Sawchenko PE & Swanson LW (1983). The organization of forebrain afferents to the paraventricular and supraoptic nuclei of the rat. *J Comp Neurol* **218**, 121–144.

Schreihofer AM, Stricker EM & Sved AF (2000). Nucleus of the solitary tract lesions enhance drinking, but not vasopressin release, induced by angiotensin. *Am J Physiol Regul Integr Comp Physiol* **279**, R239–R247.

Sly DJ, McKinley MJ & Oldfield BJ (2001). Activation of kidney-directed neurons in the lamina terminalis by alterations in body fluid balance. *Am J Physiol Regul Integr Comp Physiol* **281**, R1637–R1646.

Stocker SD, Hunwick KJ & Toney GM (2005). Hypothalamic paraventricular nucleus differentially supports lumbar and renal sympathetic outflow in water-deprived rats. *J Physiol* **563**, 249–263.

Stocker SD, Schiltz JC & Sved AF (2004). Acute increases in arterial blood pressure do not reduce plasma vasopressin levels stimulated by angiotensin II or hyperosmolality in rats. *Am J Physiol Regul Integr Comp Physiol* **287**, R127–R137.

Stocker SD, Stricker EM & Sved AF (2001). Acute hypertension inhibits thirst stimulated by ANG II, hyperosmolality, or hypovolemia in rats. *Am J Physiol Regul Integr Comp Physiol* **280**, R214–R224.

Stocker SD, Stricker EM & Sved AF (2002). Arterial baroreceptors mediate the inhibitory effect of acute increases in arterial blood pressure on thirst. *Am J Physiol Regul Integr Comp Physiol* **282**, R1718–R1729.

Tanaka J, Kaba H, Saito H & Seto K (1986). Subfornical organ efferents influence the activity of median preoptic neurons projecting to the hypothalamic paraventricular nucleus in the rat. *Exp Neurol* **93**, 647–651.

Tanaka J, Nomura M, Kariya K, Nishimura J & Kimura F (1993). Median preoptic neurons projecting to the hypothalamic paraventricular nucleus are sensitive to blood pressure changes. *Brain Res* **605**, 338–341.

Tanaka J, Saito H & Kaba H (1987). Subfornical organ and hypothalamic paraventricular nucleus connections with median preoptic nucleus neurons: an electrophysiological study in the rat. *Exp Brain Res* **68**, 579–585.

Tanaka J, Ushigome A, Matsuda M & Saito H (1995). Responses of median preoptic neurons projecting to the hypothalamic paraventricular nucleus to osmotic stimulation in Wistar-Kyoto and spontaneously hypertensive rats. *Neurosci Lett* **191**, 47–50.

Weiss ML, Claassen DE, Hirai T & Kenney MJ (1996). Nonuniform sympathetic nerve responses to intravenous hypertonic saline infusion. *J Auton Nerv Syst* **57**, 109–115.

Weiss ML & Hatton GI (1990). Collateral input to the paraventricular and supraoptic nuclei in rat. I. Afferents from the subfornical organ and the anteroventral third ventricle region. *Brain Res Bull* **24**, 231–238.

Westerhaus MJ & Loewy AD (1999). Sympathetic-related neurons in the preoptic region of the rat identified by viral transneuronal labeling. *J Comp Neurol* **414**, 361–378.

Xu L & Sved AF (2002). Acute sympathoexcitatory action of angiotensin II in conscious baroreceptor-denervated rats. *Am J Physiol Regul Integr Comp Physiol* **283**, R451–R459.

Yasuda Y, Honda K, Negoro H, Higuchi T, Goto Y & Fukuda S (2000). The contribution of the median preoptic nucleus to renal sympathetic nerve activity increased by intracerebroventricular injection of hypertonic saline in the rat. *Brain Res* **867**, 107–114.

Zardetto-Smith AM, Thunhorst RL, Cicha MZ & Johnson AK (1993). Afferent signaling and forebrain mechanisms in the behavioral control of extracellular fluid volume. *Ann N Y Acad Sci* **689**, 161–176.

Acknowledgements